THE ASTROPHYSICAL JOURNAL, 445:173–181, 1995 May 20

THE RELATIVISTIC ISM IN M33: ROLE OF THE SUPERNOVA REMNANTS

N. DURIC,[1,2] S. M. GORDON,[3] W. M. GOSS,[4] F. VIALLEFOND,[5] AND C. LACEY[1]

Received 1994 August 15; accepted 1994 November 21

ABSTRACT

The role of supernova remnants in producing and maintaining the relativistic interstellar medium is investigated for the case of the nearby galaxy M33. Analysis of a radio continuum sample of supernova remnants (SNRs) has led to the following results. (1) The SNRs use roughly 1%–10% of their blast energy to produce relativistic particles. (2) The currently observed SNR population contains between 0.1% and 1% of the relativistic particle energy of the entire interstellar medium of M33, which leads to reasonable values of the particle residence time in the disk. (3) The distribution of synchrotron spectral indices indicates that the particle populations of the observed SNRs have energy spectra with power-law indices of 2.2 ± 0.4, consistent with values predicted by diffusive shock acceleration theory. Taken together, the three results favor the hypothesis that SNRs account for the bulk of M33's relativistic medium. It is further shown that, as a consequence of these results, the predicted SN rate is 1 per 140–250 yr, in general agreement with independent estimates of the SN rate and the absence of historical supernovae.

Subject headings: acceleration of particles — galaxies: individual (M33) — galaxies: ISM — radio continuum: ISM — stars: statistics — supernova remnants

1. INTRODUCTION

It is now well established that all disk galaxies have relativistic gas as a major constituent and that this gas plays an important role in the chemical and kinematical evolution of individual galaxies. In our Galaxy, the relativistic gas contributes as much energy density as the interstellar magnetic field and the thermal gas. This equipartition of energies is probably a feature of most disk galaxies (e.g., Duric 1988, 1989). For this reason, the relativistic gas is at the root of many contemporary problems in astrophysics, such as the radio–far-infrared (FIR) correlation of galaxies, the formation of cosmic-ray (CR) halos, the nature of starbursts and active galactic nuclei (AGNs) and, of course, the origin of the relativistic gas, itself. In this paper we address the issue of the origin of relativistic gas in the nearby galaxy M33.

Previous studies of relativistic gas in disk galaxies have taken two basic approaches. The first utilizes integrated properties of galaxies and is essentially a statistical study of samples of galaxies. The radio–FIR correlation (Wunderlich, Klein, & Wielebinski 1987) is a good example of this approach. It has been argued that the remarkably tight correlation between a presumed indicator of star formation (the FIR) and an indicator of CR electrons (radio synchrotron emission) represents a physical relationship between star formation and CR production (Harwit & Pacini 1975). The scenario that has evolved from this argument is that supernova remnants (SNRs) produced by Type II supernovae (SNe) (resulting from recently formed high-mass stars) explosions produce relativistic particles through their interactions with the interstellar medium (Volk 1989; Condon, Anderson, & Helou 1991; Helou & Bicay 1993; Xu, Lisenfeld, & Volk 1994).

The second approach entails analyzing and comparing light profiles in individual galaxies. Comparisons between optical light distributions at various wavelengths and high-resolution radio continuum images have been used to correlate stellar populations with the relativistic gas (e.g., Duric et al. 1986; Condon 1992). Although this has led to opposing conclusions, recent results suggest that Hα and radio continuum distributions correlate the best (Duric & Glenn 1991). Thus, there is an implied relation between the extreme population I stars and the relativistic gas (the latter represented by the synchrotron-emitting electrons).

The two different approaches have yielded similar results in that they have established a plausible relationship between star formation and the relativistic gas in disk galaxies. There is little doubt that this relationship is real. However, the physical chain of events that leads to the production of the relativistic medium can only be inferred from these studies; it cannot be directly demonstrated. In particular, the connection between SNRs and the production of relativistic particles needs to be more closely examined and that is the goal of this paper.

The most favored hypothesis of the origin of this relativistic gas combines SNRs with the theory of diffusive shock acceleration or DSA (e.g., Bell 1978; Axford 1981; Drury 1983; Blandford & Eichler 1987; Jones & Kang 1993). A SN explosion is believed to typically release in excess of 10^{51} ergs of energy, much of which is carried by the subsequent SNR in the form of kinetic energy. The rapid expansion of the SNR causes the SNR to couple with the interstellar medium (ISM) through a supersonic shock. According to the DSA theory, particles can be accelerated at the shock front to CR energies. It is this coupling which allows the SNR to convert some of its kinetic energy into relativistic particles. If the SNRs are to be the primary souce of CRs they must provide sufficient energy to maintain the observed relativistic medium. Thus, there must be a sufficient number of SNe to be able to continuously replenish the relativistic medium over the duty cycle of the medium. Consider, for example, a relativistic medium of a disk galaxy

[1] Institute for Astrophysics, University of New Mexico, Albuquerque, NM 87106.
[2] Department of Physics, Queen's University, Kingston, Ontario Canada K71 3N6.
[3] Harvard-Smithsonian Center for Astrophysics, 60 Garden St, Cambridge, MA 02138.
[4] National Radio Astronomy Observatory, P.O. Box 0, Socorro, NM 87801.
[5] Observatoire de Paris, Section de Meudon, F-92190 Meudon, France.

that has an energy (kinetic energy of all the relativistic particles) of 10^{55} ergs and which escapes from the disk over a time of 10^7 yr. The energy needed to maintain the relativistic medium is 10^{48} ergs yr^{-1}. This requires the energy of 10^4 SNe over the duty cycle of the relativistic medium of 1 SN per 10^3 yr. However, it is unlikely that an SN converts all of its energy into relativistic particles. The conversion efficiencies are not known. A conversion efficiency of 1%, for example, would require a SN rate of 1 every 10 yr. Thus the ability of SNRs to maintain the relativistic medium depends on the required energetics. This is the primary test of the hypothesis that we discuss in this paper.

The DSA theory predicts the shape of the energy spectrum of the particles accelerated at shock fronts. Synchrotron theory allows the determination of the electron energy spectrum from the synchrotron spectrum. If the radio emission of SNRs is dominated by freshly accelerated electrons, then the observed synchrotron spectrum should probably be flatter than that of the more evolved electrons in the disk of M33. The disk electrons have undergone energy losses, most of which tend to steepen the spectrum. Comparing observed synchrotron spectral indices of SNRs with those predicted by the DSA mechanism forms the basis of an additional test of the hypothesis.

In § 2 we describe the SNR data set and the conversion of measured quantities into physical parameters relevant to the analysis. The physical parameters, derived in § 2, are used to test the SNR hypothesis in § 3. A general discussion of the role SNRs play in the maintenance of the relativistic ISM (RISM) is presented in § 4.

2. THE SNR DATA SET

2.1. *The Measured Quantities*

The optimal way in which to apply the tests to the above hypothesis is by studying a large number of SNRs. Statistical studies of SNRs in our own Galaxy are difficult to perform (Green 1991). The most efficient way to detect Galactic SNRs is through radio continuum surveys because other spectral regimes are subject to either considerable obscuration or confusion toward the galactic plane. However, flux-limited radio surveys lead to severe biases in the Galactic SNR sample because luminous SNRs are taken from larger volumes than the less luminous SNRs. Furthermore, distances are difficult to estimate with radio data alone and require indirect methods, at best. For the purpose of building a distance-limited sample of SNRs, it is desirable to observe external galaxies for which all SNRs are at essentially the same distance. For a summary of extragalactic SNR observations see Gordon (1994) and references therein. Our VLA[6]-WSRT[7] survey of M33 was motivated by these considerations. The survey is discussed in detail in Duric et al. (1993). The number of radio-detected SNRs has risen from the 26 first reported in Duric et al. (1993) to 53 (reported in Gordon 1994). The increase is primarily due to the availability of a larger optical survey of M33 allowing a greater number of radio sources to be confirmed as SNRs. Spectral information was determined for 43 SNRs. For a complete discussion of biases and completeness issues see Gordon (1994). Table 1 summarizes the new observations of SNRs.

As shown in Table 1, the basic parameters that were obtained for the SNRs are the 20 cm integrated flux density, the synchrotron spectral index between 6 cm and 20 cm, and the diameter of the SNR (estimated from the optical data). These data represent the essential parameter set used in this study. The transformation of these parameters into physical quantities relating to the properties of the relativistic gas in SNRs is discussed below.

The data used to characterize the general relativistic medium of M33 were taken from Buczilowski (1988). These data consist of Bonn single-dish measurements used to map the disk of M33 at a number of frequencies. The data relevant to our analysis are summarized in Table 2. A distance to M33 of 840 kpc was assumed throughout (Freedman, Wilson, & Madore 1991).

2.1.1. *Explanation of Table 1*

Col. (1).—The sequential ID number; col. (2).—the position-defined ID number; col. (3).—the right ascension (1950 epoch); col. (4).—the declination (1950 epoch); col. (5).—the SNR diameter in parsecs; col. (6).—the integrated flux density of the SNR at 20 cm; col. (7).—the uncertainty in the measured flux density; col. (8).—the synchrotron spectral index, α, determined from the 6 cm and 20 cm flux densities using the convention, $S_\nu \propto \nu^{-\alpha}$; col. (9).—the uncertainty in α calculated using propagation of 6 cm and 20 cm flux errors; col. (10).—the minimum nonthermal energy of the SNR, as calculated below.

2.1.1. *Explanation of Table 2*

Col. (1).—The integrated 20 cm flux density; col. (2).—the 20 cm flux density corrected for thermal emission; col. (3).—the spectral index of the integrated radio emission; col. (4).—the spectral index of the nonthermal emission (corrected for thermal emission); col. (5).—the exponential scale length of the nonthermal disk; col. (6).—the assumed exponential scale height; col. (7).—the minimum energy in particles and fields (§ 2.2).

2.2. *The Physical Properties of the SNRs*

Whether SNRs are able to maintain the RISM depends on how much of their energy goes into relativistic particle production. Determining whether particles are accelerated via the DSA mechanism depends, in part, on how well the predicted particle spectra agree with those inferred from the observations. We now describe the conversion of the observables into parameters that can be used to address these questions.

From synchrotron theory it is possible to determine the minimum energy in relativistic particles and magnetic fields needed to power a SNR as a radio source. For a spherical shell geometry of diameter, D, the nonthermal energy is given by

$$U = U_{cr} + U_B = aB^{-3/2} + bB^2$$
$$= c_0(\alpha, \nu_1, \nu_2)(K+1)^{4/7}\phi^{3/7}D^{9/7}L^{4/7}, \quad (1)$$

where a and b are constants, B is the magnetic field strength. The radio luminosity, L, is given by $L = 4\pi d^2 \int_{\nu_1}^{\nu_2} S_\nu \, d\nu$, where d is the distance to the SNR and S_ν is the flux density as a function of frequency. The quantity c_0 is a slowly varying function of the synchrotron spectral index, α, the frequency cutoffs, ν_1 and ν_2, the assumed value of K, the ratio of relativistic nuclei to electrons, and the filling factor, ϕ (e.g., Pacholczyk 1970). Without knowledge of B, the energy residing in relativistic

[6] The National Radio Astronomy Observatory is operated by Associated Universities, Inc., under cooperative agreement with the National Science Foundation.

[7] The Westerbork Synthesis Radio Telescope is operated by the Netherland Foundation for Research in Astronomy (NFRA) with financial support from the Netherland Organization for the Advancement of Research (NWO).

TABLE 1

RADIO CONTINUUM PROPERTIES OF THE SUPERNOVA REMNANTS

ID. #	SNR ID	RA 1950	DEC 1950	D (pc)	S_{20} (mJy)	δS_{20} (mJy)	α	$\delta\alpha$	U_{min} (10^{50} ergs)
1	004+228	1:30:04.0	30:22:49	57.9	0.89	0.23	>	0.37	1.31
2	007+252	1:30:07.3	30:25:13	88.7	1.01	0.17	0.64	0.23	2.50
3	008+241	1:30:08.3	30:24:04	24.1	0.72	0.21	0.51	0.31	0.36
4	015+245	1:30:15.0	30:24:30	44.9	0.62	0.13	0.31	0.27	0.77
5	021+241	1:30:21.0	30:24:08	67.0	2.32	0.20	0.53	0.13	2.65
6	022+190	1:30:22.2	30:18:59	67.8	0.68	0.28	0.45	0.46	1.32
7	022+244	1:30:22.3	30:24:21	20.9	0.84	0.15	0.66	0.26	0.36
8	040+269	1:30:40.0	30:26:55	29.1	0.80	0.17	0.24	0.22	0.53
9	042+182	1:30:42.2	30:18:11	37.3	1.75	0.13	0.75	0.14	1.25
10	047+211	1:30:46.8	30:21:05	30.3	3.48	0.15	0.68	0.07	1.32
11	059+177	1:30:58.8	30:17:43	40.4	0.20	0.13	>	-1.33	0.35
12	101+201	1:31:00.6	30:20:04	44.6	0.59	0.16	0.72	0.46	0.82
13	102+285	1:31:02.1	30:28:31	54.4	0.42	0.10	-0.00	0.26	1.07
14	105+189	1:31:05.4	30:18:26	52.4	0.20	0.08	>	-0.75	0.49
15	106+178	1:31:05.8	30:17:49	23.3	4.43	0.19	0.73	0.06	1.13
16	108+196	1:31:07.9	30:19:37	23.3	0.37	0.12	0.90	0.72	0.34
17	109+168	1:31:09.0	30:16:48	23.4	0.26	0.09	>	-0.43	0.20
18	110+182	1:31:09.7	30:18:13	29.7	0.35	0.10	0.01	0.33	0.44
19	111+270	1:31:11.0	30:26:59	33.4	0.52	0.12	0.23	0.21	0.50
20	113+157	1:31:13.3	30:15:43	53.2	0.56	0.15	0.79	0.51	1.08
21	114+294	1:31:14.2	30:29:22	43.4	0.59	0.10	>	0.40	0.72
22	121+271	1:31:21.4	30:27:04	23.4	0.51	0.07	1.10	0.39	0.59
23	127+176	1:31:26.5	30:17:37	33.4	0.43	0.10	0.43	0.29	0.41
24	128+261	1:31:28.2	30:26:03	52.4	0.39	0.07	0.53	0.25	0.70
25	035+108	1:30:34.8	30:10:49	33.0	1.43	0.19	0.86	0.20	1.09
26	152+281	1:31:51.6	30:28:08	43.6	0.81	0.11	0.14	0.15	0.99
27	942+123	1:29:41.6	30:12:17	107.5	4.95	0.69	0.51	0.14	7.46
28	953+055	1:29:52.5	30:05:27	87.0	2.26	0.56	0.51	0.23	3.63
29	011+287	1:30:11.2	30:28:43	20.8	0.62	0.18	>	-0.20	0.29
30	015+160	1:30:14.5	30:15:58	35.2	1.12	0.17	0.81	0.25	0.97
31	022+233	1:30:22.4	30:23:19	21.5	0.90	0.16	0.72	0.26	0.41
32	029+161	1:30:28.6	30:16:05	31.7	0.30	0.09	>	-0.30	0.33
33	034+117	1:30:33.6	30:11:41	21.0	1.76	0.20	0.43	0.12	0.50
34	038+324	1:30:37.5	30:32:25	40.7	0.68	0.21	>	0.21	0.72
35	039+162	1:30:39.0	30:16:12	29.1	1.21	0.14	0.76	0.21	0.74
36	040+338	1:30:40.2	30:33:47	28.1	0.54	0.12	0.84	0.46	0.50
37	041+322	1:30:40.7	30:32:11	28.1	0.42	0.17	0.53	0.52	0.33
38	049+166	1:30:48.6	30:16:38	20.9	0.39	0.07	0.72	0.29	0.24
39	051+369	1:30:51.4	30:36:51	58.3	0.48	0.09	1.11	0.69	1.86
40	052+058	1:30:52.4	30:05:45	41.7	1.33	0.26	0.76	0.28	1.25
41	054+257	1:30:54.0	30:25:44	26.0	1.16	0.10	0.59	0.16	0.54
42	103+157	1:31:02.8	30:15:39	54.2	0.65	0.08	0.77	0.25	1.17
43	106+300	1:31:05.5	30:29:58	23.2	1.29	0.07	0.85	0.12	0.65
44	108+254	1:31:07.8	30:25:25	26.6	1.09	0.10	0.99	0.15	0.87
45	140+261	1:31:40.3	30:26:04	52.4	0.82	0.11	0.40	0.18	1.06
46	141+204	1:31:40.6	30:20:24	52.4	0.31	0.06	0.90	0.43	0.88
47	109+365	1:31:09.3	30:36:30	39.6	0.29	0.09	>	-0.23	0.42
48	943+201	1:29:42.5	30:20:07	36.9	0.27	0.13	0.36	0.54	0.36
49	100+241	1:30:59.8	30:24:05	24.7	0.31	0.05	0.21	0.24	0.26
50	127+375	1:31:27.1	30:37:29	111.3	1.75	0.20	0.43	0.12	4.28
51	115+176	1:31:15.0	30:17:37	33.0	0.37	0.07	0.50	0.32	0.37
52	050+211	1:30:49.7	30:21:03	53.8	0.20	0.07	>	-0.12	0.51
53	052+170	1:30:51.7	30:17:00	27.5	0.51	0.13	0.75	0.35	0.42

TABLE 2

INTEGRATED PROPERTIES OF THE RELATIVISTIC INTERSTELLAR MEDIUM IN M33

S(20 cm)	S_{nth}(20 cm)	α	α_{nth}	U (ergs)	$R(kpc)$	$h(kpc)$
3.0 ± 0.4	2.7 ± 0.4	0.9 ± 0.1	1.1 ± 0.1	1.5×10^{54}	4.3 ± 0.3	1.0

particles cannot be uniquely determined unless the SNR is at the minimum energy. In that case,

$$dU/dB = 0 \rightarrow U_{cr} = 4/3U_B \rightarrow U_{cr} = 4/7U_{min} ,$$

and there is an approximate equipartition of energy between the particles and the field. Consequently the energy in particles and the field can be evaluated so that $U_{cr} = 4/7c_0 D^{9/7} L^{4/7}$ and $B_0 = c_1 D^{-6/7} L^{2/7}$. The uncertainties in the calculation of U_{cr} arising from variations in ν_1, ν_2, K, and ϕ are discussed fully in § 2.3, below. With these uncertainties in mind, the quantity U_{cr} can be determined for each SNR from the observed values of α, D, and S_ν and is listed in Table 1. Some SNRs were detected only at one frequency and for these the mean spectral index, $\alpha = 0.6$, was used (Fig. 3).

The energy in the RISM was calculated from the observations listed in Table 2 using similar assumptions. The scale lengths from Table 2 were used to estimate the emitting volume of the disk (the effective volume occupied by the relativistic gas). The nonthermal spectral index of the integrated emission was used to characterize the spectral properties of the relativistic electrons. The calculated value of the minimum energy, U_D, is listed in Table 2.

An ensemble of relativistic electrons with a differential energy spectrum of the form

$$N_e(E) = N_0 \left(\frac{E}{E_0}\right)^{-\gamma} \quad (2)$$

radiating in a magnetic field will produce a synchrotron spectrum of the form

$$S(\nu) = S_0 \left(\frac{\nu}{\nu_0}\right)^{-\alpha} , \quad (3)$$

also a power law. There is a one-to-one relationship between the power-law index γ and the synchrotron spectral index, α, such that

$$\gamma = 2\alpha + 1 . \quad (4)$$

Thus, the spectral indices listed in Table 1 can all be converted to γ's via equation (4). Similarly, the γ of the electrons in the disk can be evaluated.

2.3. *Uncertainties*

The derived parameters have uncertainties resulting from measurement error and effects of simplifying assumptions. In the case of the minimum energy calculations the uncertainties arising from the assumptions dominate all other errors.

Since spectral data on the SNR flux densities is limited to the two observing frequencies, the cutoffs had to be assumed. The standard values of 10^7 and 10^{11} Hz were assumed for ν_1 and ν_2, respectively. In practice, only the lower frequency cutoff contributes significantly to the equipartition calculations. Electrons radiating in magnetic fields of a few times 10^{-5} G at 10^7 Hz have energies of $\approx$300 MeV. It is not known at what energies the electron (and proton) energy spectra turn over but a firm lower limit on the electrons would be in the neighborhood of 0.5 MeV, the rest mass energy of the electron which would correspond to $\nu_1 \approx 30$ Hz. A variation of ν_1 from 30 Hz to 10^7 Hz yields a variation in U_{cr} of only a factor of 2. As discussed below, this is much less than the variation possible from departures from equipartition. The dependence of U_{cr} on K is more sensitive. The value of K measured at the Earth, and used in these calculations, is $\approx$40. However, values motivated by theory range from 1 to 100. Such a variation in K yields an order of magnitude change in U_{cr}. In this analysis, it is only the *relative* values of K between the disk and the SNRs that is important. Barring any strong evolution of K in the disk of M33, the results of the analysis on § 3.2 should not depend strongly on the adopted value of K. The filling factor ϕ was assumed to be 0.25, corresponding to a simple shell geometry in which the accelerated particles are assumed to populate the downstream region of a spherical, adiabatic shock. Observations of Galactic SNRs suggest that filling factors typically range from 0.1 to 1. Such a variation in ϕ leads to a variation in U_{cr} of less than 3.

The greatest source of uncertainty is the equipartition assumption itself. The temporal and spatial scales over which particles and fields come into energy equipartition are not well known. Equipartition is likely to hold for the disk as a whole as suggested by independent measurements of CR fluxes and interstellar magnetic field energy densities in our Galaxy (for review see Longair 1986) and by the similarities in the distributions of γ-ray and radio continuum distributions along the Galactic plane (e.g., Haslam et al. 1981). However, it is far less likely that equipartition holds for small dynamic systems like SNRs which are presumably actively producing relativistic particles. Still, a system that is not in equipartition is also not in a minimum energy configuration. Furthermore, as equation (1) indicates, the total nonthermal energy in particles and fields is a strong function of the magnetic field B. Thus any significant change of B from its equipartition value causes a corresponding nonlinear increase in the total energy U. The increase in total energy occurs either at the expense of the magnetic field energy or the particle energy. Significant departures from equipartition therefore lead to the dominance of either the field or the particles and quickly lead to physical untenable scenarios for powering the radio source. There is therefore a limited range of values of U that can reasonably power a radio source such as a SNR. This limitation is quantified below in § 3.

The primary source of uncertainty in the spectral index determinations is the measurement error associated with the flux densities of the SNRs at 6 cm and 20 cm (Table 1). The errors in α were calculated using standard error propagation. We now discuss the statistical properties of the SNR sample in light of these uncertainties with the goal of testing the hypothesis.

3. TESTING THE HYPOTHESIS

3.1. *Relativistic Particle Yield of SNRs*

The hypothesis that SNRs are the primary source of the RISM can be tested by estimating the capacity of SNRs to produce relativistic particles. As noted above, the minimum

energies of the SNRs provide potential information on the relativistic particles that they contain. A histogram of minimum energies, based on the entries in Table 1, is shown in Figure 1. The minimum energy distribution peaks at $U = 5 \times 10^{49}$ ergs and has a half-width of $\Delta U = 2 \times 10^{49}$ ergs. The histogram is estimated to be incomplete for $U \leq 2 \times 10^{49}$ ergs. Adopting an average value of $U \approx 5 \pm 2 \times 10^{49}$ ergs allows us to estimate the efficiency of converting SNR kinetic energy into relativistic particles and fields. For a typical kinetic energy of $E_0 = 10^{51}$ ergs, the estimated efficiency is 5% ± 2%. Given that U is the *minimum* energy, the quoted efficiency is a lower limit. Thus at least 5% of the kinetic energy of a typical SNR in our sample is converted into particles and fields.

The question of how this efficiency translates into an efficiency of relativistic particle production cannot be directly answered without making some assumptions about the relative energy in particles versus the magnetic field. Under a straightforware equipartition argument, the efficiency ζ can be defined as $\zeta = (4/7)U/E_0$. Using the above numbers a typical value of 3% ± 1% results, suggesting that roughly 3% of the kinetic energy is converted into relativistic particles.

If equipartition does not hold, there are two extreme possibilities to examine. In the first, magnetic field energy dominates the particle energy, $U_B \gg U_{cr}$. In this case, $U \approx U_B \propto B^2$. For example, a factor of 2 increase in magnetic field strength over its equipartition value leads to $U \approx 0.1E_0$ while $U_{cr} \approx 0.01E_0$. Any further increase in magnetic field strength leads to magnetic energies comparable to the kinetic energy, a physically untenable situation. Furthermore, such high B fields place the SNRs well into the van der Laan regime (van der Laan 1962) which is generally believed to be only relevant for old SNRs with radiative shocks, a feature that does not apply to the SNRs in this sample (Long et al. 1990; Gordon 1994). Assuming therefore that $U_B \leq 0.1E_0$ leads to a lower limit for $U_{cr} > 0.01E_0$ or a lower limit on the efficiency, $\zeta > 1\%$. At the other extreme, $U_{cr} \gg U_B$. For a SNR in the Sedov-Taylor stage of expansion a shock compression ratio of $\chi \approx 4$ is expected. Thus, the ambient magnetic field, $B_0 \approx 5\mu$G, should be compressed by this factor resulting in a minimum SNR field of $4B_0$ or 20 μG. The corresponding magnetic field energy constrains the particle energy, U_{cr} to $0.1E_0$.

We conclude that the widest possible range of values for the efficiency of relativistic particle production is given by $0.01 < \zeta < 0.1$. This range allows for significant departures from equipartition. The corresponding range in U_{cr} is $10^{49} < U_{cr} < 10^{50}$ ergs for the *typical* remnant in our sample with the equipartition value corresponding to $U_{cr} \approx 3 \times 10^{49}$ ergs. The range of ζ is consistent with predictions of DSA theory (Drury, Markiewicz, & Volk 1989); Kang & Drury 1990; Jones & Kang 1993).

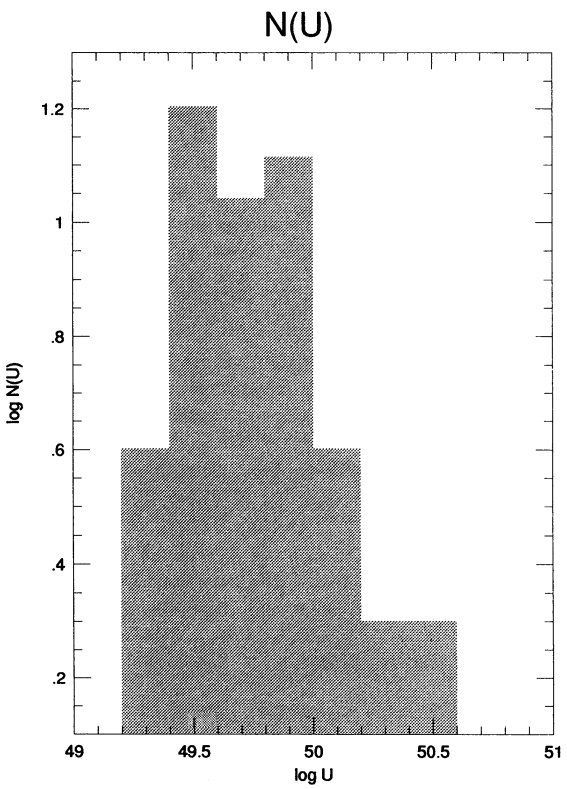

FIG. 1.—The histogram of SNR minimum energies (ergs). The equipartition CR energies, U_{cr}, are obtained through the relation, log U_{cr} = log U − log (4/7).

3.2. *Replenishment of the Relativistic ISM*

To determine the total U in all SNRs requires an estimate of the quantity

$$U_\Sigma = \int_0^\infty UN(U)\,dU\ . \tag{5}$$

For a power law $N(U)$ distribution, the integrand is related to the cumulative function $N(>U)$ which is shown in Figure 2 in the form of a histogram. As noted earlier, the sample is incomplete for log $U \leq 49.2$ and this can be seen as a complete flattening of $N(>U)$. Another break point occurs near log $U = 49.9$. If taken as a real break (see discussion in § 4 regarding possible incompleteness), the distribution can be approximated as two power laws, one representing log $U \geq 4.9$ (index = −1.5), the other the range $49.2 <$ log $U < 49.7$ (index = −0.8). The fits were obtained via a maximum likelihood method (e.g., Crawford, Jauncey, & Murdoch 1970). Extrapolating the latter range to $U = 0$ and the former to $U = \infty$ leads to a complete definition of the integrand in equation (5). Evaluation of the integral leads to an estimate of $U_\Sigma \approx 8 \times 10^{51}$ ergs. A single power-law fit (index = −0.9) yields $U_\Sigma \approx 10^{52}$ ergs. A simple sum of the histogram in Figure 1 yields $U_\Sigma \approx 5 \times 10^{51}$ ergs. We estimate that incompleteness may affect these estimates by no more than a factor of 2 (see discussion in § 4 and Gordon 1994).

We now define the fraction, f, of minimum nonthermal energy in *all* SNRs relative to the minimum energy in all of M33,

$$f = \frac{U_\Sigma}{U_D}\ . \tag{6a}$$

Using the value of U_D from Table 2 yields $f = 5 \times 10^{-3}$. The corresponding fraction of the particle energy alone is given by

$$f' = \frac{7}{4}\frac{U'_\Sigma}{U_D}\ , \tag{6b}$$

where U'_Σ is the energy in relativistic particles alone. Under equipartition assumptions, $f = f'$, so that only 0.5% of the relativistic particles in M33 are in SNRs. Under nonequipartition conditions, f' deviates from f (see discussion in § 3.1). If the

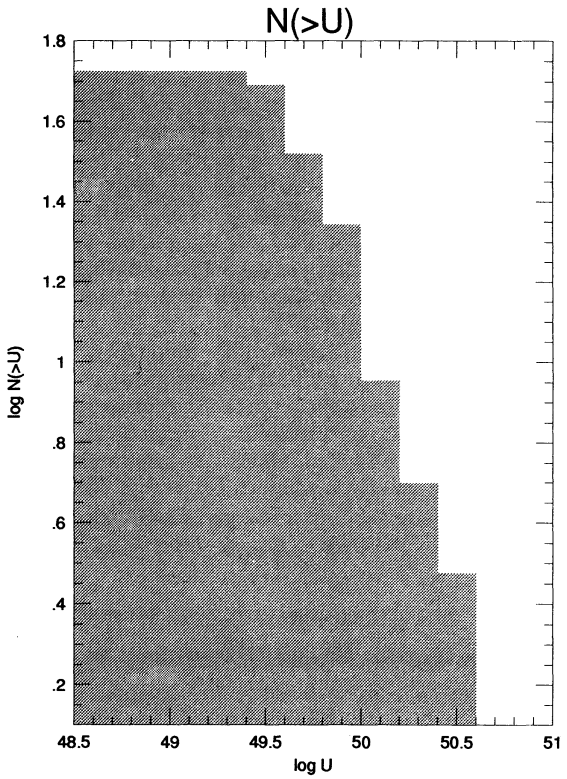

FIG. 2.—The cumulative number energy relation corresponding to the histogram in Fig. 1. Two power laws were fitted on the basis that there is an apparent break in the luminosity function. For $49.2 < \log U < 49.7$ and for $49.7 < \log U < 50.3$ the power-law index was found to be -0.8 and -1.5, respectively. The region below 49.2 is known to be incomplete. A single power-law fit yields an index of -0.9. The fits were performed using a maximum likelihood method (Crawford et al. 1970). Both methods generated similar values of U_Σ.

SNR nonthermal energies are dominated by the magnetic field, $f' = 10^{-3}$. Conversely, if particles dominate, $f' = 10^{-2}$. The possible range is therefore

$$10^{-3} < f' < 10^{-2} . \tag{7}$$

We now address the question of whether this range of f' allows SNRs to be the primary source of the relativistic ISM in M33.

Consider a simple model in which SNRs are the sole injectors of relativistic particles in the disk of M33. Particles are injected on the timescale of the SNR lifetime, $\tau_{\rm snr}$. A number of arguments have been made that the acceleration timescale should correspond to the Sedov-Taylor expansion phase because that is the phase in which particle acceleration is thought to be the most efficient. Estimates of such a timescale range from 10^4 to 5×10^4 years (Smith 1991; Woltjer 1972; Gordon 1994). We adopt a value of 2×10^4 yr in this analysis (corresponding to the oldest SNRs in the Sedov-Taylor phase in the M33 sample; see Smith 1991 and Gordon 1994). The other important timescale is that over which the RISM would dissipate in the absence of new particles. In CR terms this is the residence time, τ_r, of the relativistic particles in the disk of M33 and is unknown.

The average rate, $\dot{U}'$, at which the SNR population produces energy in the form of relativistic particles can be expressed as

$$\dot{U}'_\Sigma = \frac{U'_\Sigma}{\tau_{\rm snr}} . \tag{8}$$

The relativistic particles escape from the disk of M33 at a rate of

$$\dot{U}'_D = \frac{4}{7}\frac{U_D}{\tau_r} . \tag{9}$$

Consider now a steady state scenario in which the energy content of the RISM is independent of time over the timescale, τ_r. Then, $\dot{U}'_\Sigma = \dot{U}'_D$ and from equation (6b)

$$\frac{U'_\Sigma}{\tau_{\rm snr}} = \frac{4}{7}\frac{U_D}{\tau_r} \rightarrow f' = \frac{\tau_{\rm snr}}{\tau_r} . \tag{10}$$

Inserting the above values for f' and $\tau_{\rm snr}$ into equation (10) yields

$$2 \times 10^6 < \tau_r < 2 \times 10^7 \text{ yr} . \tag{11}$$

It is interesting to note that this range overlaps with the residence time of 6×10^6–2×10^7 years estimated for our Galaxy (Gaisser 1990 and references therein). The value obtained for the equipartition case is $\tau_r = 4 \times 10^6$ yr. The relative agreement with the Galactic value supports the hypothesis posed earlier that SNRs are able to maintain the relativistic medium of M33.

3.3. *Spectra of Accelerated Particles in the SNRs*

The one-dimensional shock acceleration theory yields the following expression for the power-law spectral index:

$$\gamma_0 = \frac{\chi + 2}{\chi - 1} , \tag{12}$$

where χ is the compression ratio of the shock. For an ideal gas subject to an adiabatic shock, χ approaches an asymptotic value of 4 with increasing Mach number. Thus γ_0 is predicted to approach a value of 2.0. The fact tht χ is close to the value of 4 for even modest values of the Mach number suggests that γ_0 should have an almost universal value of 2.0.

A histogram of spectral indices is shown in Figure 3. The mean value is 0.61 ± 0.05 and the distribution has a width of 0.4. The breadth of the distribution is almost certainly the result of measurement errors (see discussion by Gordon 1994). Nevertheless, the typical SNR spectral indices are significantly flatter than the spectral index of 1.0 ± 0.1 characteristic of the RISM (Table 2). Converting the synchrotron spectral indices to energy spectral indices yields $\gamma = 2.2 \pm 0.4$ (eq. [4]). This value of γ is reasonably close to the predicted value of 2.0 based on the simple one-dimensional theory. However, SNR shocks are not one-dimensional and this acts to reduce the predicted value of χ and increase the value of γ_0. On the other hand, if the shock is radiative, χ is increased and γ_0 correspondingly decreased. Both of these effects may be found in our data and could account for some of the dispersion in the distribution. We conclude that the observed histogram of spectral indices is consistent with predictions of the DSA theory allowing for measurement error and departures from one-dimensional and possibly nonadiabatic conditions for some SNRs in the sample.

However, it is important to note that the above result does not constitute a proof that we are, in fact, observing the freshly accelerated electrons. Anderson & Rudnick (1993) have pointed out, on the basis of their analyses of Galactic SNRs, that the electrons seen in the radio observations are not necessarily those currently being accelerated. Nevertheless, the

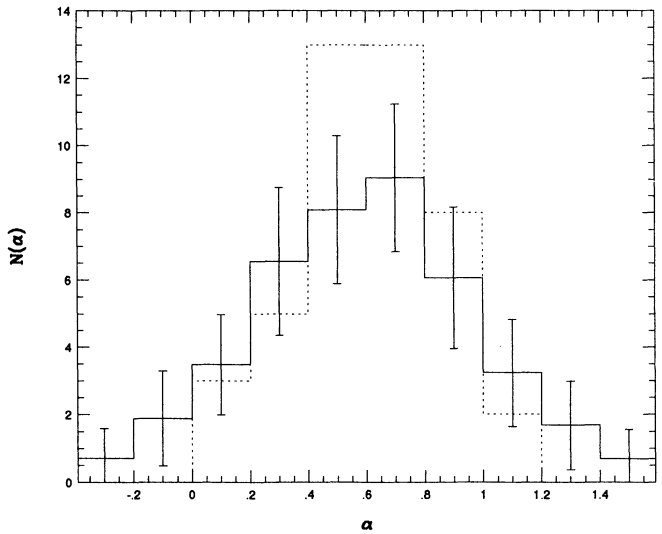

FIG. 3.—The histogram of spectral indices for the SNR sample. The dashed curve represents the binned spectral indices. The solid line represents binning according to a Monte Carlo simulation of the means and uncertainties in each bin. The horizontal line in each bin is the average while the error bars are the standard deviations determined from 100 simulations produced by the Monte Carlo bootstrap method. We assumed that the observed spectral index distribution is representative of the true underlying distribution. Each of the simulations was produced by selecting a spectral index from the observed sample and adding a random increment based upon the observed error. This was repeated 53 times to generate one simulation.

observed electrons are still those that the SNR will inject into the ISM. If that is the case, then it is important to understand the difference between the spectral properties of the SNR electrons and the electrons in the ISM.

Semiempirical propagation models, used to describe Galactic CRs (Ginaburg et al. 1980), indicate that particles diffuse with an energy-dependent diffusion coefficient such that

$$D(E) = D_0\left(\frac{E}{1\ \mathrm{GeV}}\right)^{\delta}, \tag{13}$$

where E is the energy of the particle and δ is typically ≈ 0.5–0.6. This leads to an evolution of the particle spectrum so that, in the absence of energy losses and in the steady state, the spectrum steepens from an initial value of γ_0 to a steady state value of $\gamma = \gamma_0 + \delta$. Using equation (4), the corresponding change in the synchrotron spectral index is $\alpha = \alpha_0 + \delta/2$. Taking α_0 to be the mean spectral index of the SNRs and α to be the index typical of the disk electrons yields a δ of 1.0 ± 0.4 (Tables 1 and 2). This agrees with the Galactic values of δ to within the errors.

However, it is likely that the electrons experience radiative losses. At the frequencies of observations, typical relativistic electron energies are $\approx$8–13 GeV. At these energies the dominant energy loss mechanisms are synchrotron and inverse Compton radiation. Both loss rates are $\propto E^2$. In a steady state where losses and diffusion work together, an equilibrium spectrum is achieved such that

$$\gamma = \gamma_0 + 0.5 + \frac{\delta}{2} \tag{14}$$

(Bloemen 1991, and references therein). Combining with equation (4) and taking the SNR spectral index to be that of the injected electrons yields

$$\alpha = \alpha_0 + 0.25 + \frac{\delta}{4}. \tag{15}$$

For $\alpha = 1.1 \pm 0.1$ and $\alpha_0 = 0.6 \pm 0.1$, $\delta = 1.0 \pm 0.4$, as above.

The evolution of the relativistic gas spectrum in the disk of M33 is consistent with a SNR origin.

4. DISCUSSION

In § 1 we posed the hypothesis that SNRs produce and maintain the relativistic ISM of M33. This hypothesis has been tested in three specific ways in § 3. The estimated CR production efficiency of 1%–10% is consistent with theoretical predictions and is in the range needed to make SNRs significant sources of relativistic particles. The ability of the SNR population of M33 to maintain the RISM is characterized by the residence time of a typical relativistic particle in the disk of M33. The order of magnitude range found for the residence time overlaps to a large extent that found for our Galaxy, lending support to the SNR hypothesis. Finally, the spectral signature of the relativistic particles inside SNRs indicates that the freshly accelerated electrons have spectral indices of $\gamma \approx 1.8$–2.6 in broad agreement with theoretical predictions of $\gamma \approx 2$. The distinctly flatter indices relative to the particles in the ambient RISM lends further support to the hypothesis that SNRs are active sites of particle acceleration. Though the result is consistent with predictions of the DSA theory, it does not by itself prove that the DSA mechanism operates in the SNRs.

Although the individual results harbor significant quantitative uncertainties, the collective results support a picture in which SNRs play a significant role in the production and maintenance of the RISM. At best, the results indicate that SNRs are the sole required source of the RISM in M33. On the basis of the latter possibility, we now discuss the SNR scenario in more general terms. We begin with a discussion of the fundamental assumptions inherent in the analyses of § 3. Then we examine the entire picture for self-consistency.

The discussion of a SNR contribution to the RISM is very dependent on the shape of the $N(U)$ function which is ultimately based on the radio luminosity function of SNRs in M33. As discussed extensively in Gordon (1994), such functions are subject to considerable selection effects and incompleteness. We have examined the role of surface brightness limits (which cause sampling of large faint SNRs to be incomplete) and the role of the finite-sized primary beams of the VLA and WSRT (which introduces radially dependent selection effects over the survey area) on the luminosity function. No major sources of bias or incompleteness were found apart from the absolute sensitivity limit of the survey (Gordon 1994). It is nevertheless possible that unforeseen sources of bias may still operate. In that case the discussion in § 2 would be affected. One way to place a limit on the incompleteness is to estimate the expected number of SNRs in the Sedov-Taylor phase and compare that with the number actually detected. Estimates of the SN rate for M33 range from 1 per 140 yr to 1 per 360 yr (see Blair & Kirshner 1985; Berkhuijsen 1987; Long et al. 1990; Smith 1991; Gordon 1994 and the discussion below). For a Sedov-Taylor lifetime of 2×10^4 yr the predicted number of SNRs in the Sedov-Taylor phase, currently resident in M33, is 55–140. The range is consistent with the number actually detected (53 in the radio and 98 optically). Since most of the detected SNRs

are believed to be in the Sedov-Taylor phase incompleteness for this class of SNR cannot be much more than about a factor of 2. Since incompleteness usually increases with fainter SNRs the missing remnants are unlikely to contribute as much to U_Σ as is already represented in the observed $N(U)$ relation. In any case, such corrections to the $N(U)$ distribution can only *increase* the nonthermal energy of the SNR population and therefore *decrease* the estimates of the residence time. Decreasing the residence time reinforces the role of SNRs in maintaining the RISM because it indicates less dependence on the disk as a reservoir.

An extreme interpretation of the nonthermal energies of individual SNRs would also compromise the discussion in § 2. If, in fact, a large fraction ($>10\%$) of the blast energy is in the form of magnetic fields, as opposed to relativistic particles (as might be expected from an extreme variant of van der Laan compression), then the minimum energy calculations have little to do with relativistic particles. Such an extreme interpretation would, however, require that most of the radio SNRs in our sample have magnetic fields in excess of 0.5 mG *averaged over the entire SNR*. The contrast between the spectral properties of the SNRs and those of the RISM also argues aganst this interpretation and in favor of the SNRs containing a distinct and separate population of relativistic particles. Finally, the studies of Smith (1991) and Gordon (1994) show that almost all of the SNRs in the sample are likely to be in the Sedov-Taylor phase of evolution. Consequently, the extreme compression ratios required in the van der Laan interpretation are not possible because the shocks are mainly adiabatic.

We now examine the self-consistency of the SNR scenario. Two fundamental timescales are involved. The first is the timescale, $\tau_{\rm snr}$, over which a SNR produces significant quantities of relativistic particles. The second is the time interval between SN explosions, the reciprocal of the SN rate, $\dot{N}$. A specific consequence of setting $\tau_{\rm snr}$ to the Sedov-Taylor timescale is that the SNRs produce relativistic particles over only a fraction of their lifetimes. One therefore expects that if the $N(U)$ relation does indeed flatten below $\log U = 49.7$ fewer than 1 SNR in 10 are currently producing significant quantities of relativistic particles. The total number of SNRs is given by

$$N = \dot{N}\tau_{\rm snr} . \tag{16}$$

The supernova rate, $\dot{N}$, can be estimated from the radio SNRs via

$$\dot{U}'_D = \dot{N}\zeta E_0 , \tag{17}$$

which represents a steady state balance between the production rate of particles and the rate of loss from M33. Keeping in mind that ζ and τ_r are correlated, equations (9), (11), and (17) yield, $\dot{N} = 0.004$–0.007 or 1 SN per 140–250 yr. This result is in agreement with a number of independent estimates of the SN rate (Blair & Kirshner 1985; Berkhuijsen 1987; Long et al. 1990; Smith 1991; Gordon 1994) and with the absence of historical SNe. Thus, $\dot{N}$ is the SN rate necessary to maintain the RISM of M33. The fact that it agrees with independent measurements of $\dot{N}$ adds further weight to the self-consistency of the hypothesis.

From the derived value of $\dot{N}$, equation (16) yields the total number of SNRs producing relativistic particles, N_R, in the Sedov-Taylor phase at any given time. Thus,

$$N_R = \dot{N}\tau_{\rm snr} \approx 80\text{–}140 ,$$

which is entirely consistent with the $N(U)$ relation found in § 3 and indicates that the observed sample represents about 40%–66% of particle-producing SNRs. This result vindicates the use of the $N(U)$ relation (Fig. 2) for calculating the residence time (the undetected SNRs contribute little to the total U and were accounted for by extrapolating the relation as described in § 3.2). Allowing for SNR evolution past the Sedov-Taylor phase and a total SNR lifetime, $\tau \approx 2 \times 10^5$ yr, the total number of SNRs currently in the disk of M33 should be $\approx$800–1400. The observed radio luminosity function of SNRs in M33 [i.e., the $N(U)$ relation] therefore represents only a small fraction of the total SNR population but includes the SNRs currently producing the bulk of the relativistic particles. Inclusion of the undetected, older SNRs would leave the estimate of the residence time unchanged because their numbers scale linearly with the assumed total SNR lifetime. So long as the post-Sedov-Taylor stage does not contribute significantly to particle production the quantity $\dot{U}'_\Sigma$ remains unchanged.

The above results suggest that the disk of M33 acts as a reservoir of CR particles. SNRs embedded in the disk inject particles into the ISM over a period of $\approx 2 \times 10^4$ yr with an energy spectrum significantly flatter than that of the disk particles. The injected particles, with a γ near 2.0, diffuse through the disk over the residence time of 2×10^6–2×10^7 yr and their spectrum equilibrates to a value close to $\gamma \approx 3.0$. The evolution of the spectrum is governed by a combination of energy-dependent diffusion and radiative energy losses.

5. SUMMARY

We have presented a systematic, quantitative evaluation of the hypothesis that the relativistic medium of M33 is fed and maintained by SNRs. Our analysis is based on extensive radio and optical surveys of M33. In this paper, three quantitative tests of the hypothesis were performed. A relativistic particle yield of a typical SNR in the sample was found to be in the range of 1%–10%. The SNR population was found to contain between 0.1% and 1% of *all* relativistic particles in M33 which leads to an estimate of the residence time of 2×10^6–2×10^7 yr. The spectral index distribution of the SNRs peaks near $\alpha = 0.6$ indicating that the relativistic electrons in SNRs have $\gamma = 2.2 \pm 0.4$. Though the numerical results have substantial uncertainties they are all consistent with a SNR origin of the relativistic gas and with the predictions of the DSA theory.

The self-consistency of the hypothsis was examined by estimating the SN rate and predicting the total number of SNRs currently residing in the disk of M33. The SN rate was found to be 1 per 140–250 yr which agrees with independent estimates of the SN rate in M33. The number of particle-producing SNRs is predicted to be $\approx$80–140, consistent with the $N(U)$ distribution and the observed radio luminosity function of SNRs. The total number of SNRs was estimated to be $\approx$800–1400. Fewer than one in 10 SNRs are predicted to be significantly accelerating particles at any given time. The brightest 40 or so SNRs are producing the bulk of the relativistic particles at the present epoch. This analysis allows the construction of a self-consistent picture in which the SNR population of M33 is the primary contributor to the production and maintenance of the relativistic ISM of M33.

N. D. acknowledges the support of NSF grant AST 90-22342 under which this work was performed. The authors thank Larry Rudnick (University of Minnesota) for his constructive comments.

REFERENCES

Anderson, M. C., & Rudnick, L. 1993, ApJ, 408, 514
Axford, W. I. 1981, Proc. 20th Int. Cosmic Ray Conf., 12, 155
Bell, A. R. 1978, MNRAS, 182, 147
Berkhuijsen, E. M. 1987, A&A, 181, 398
Blair, W. P., & Kirshner, R. P. 1985, ApJ, 289, 582
Blandford, R. D., & Eichler, D. 1987, Phys. Rep., 154, 1
Bloemen, H. 1991, in Interpretation of Modern Synthesis Observations of Spiral Galaxies, ed. N. Duric & P. C. Crane (ASP Conf. Ser. 18), 27
Buczilowksi, U. R. 1988, A&A, 205, 29
Condon, J. J. 1992, ARA&A, 30, 575
Condon, J. J., Anderson, M. L., & Helou, G. 1991, ApJ, 376, 95
Crawford, D. F., Jauncey, D. L., & Murdoch, H. S. 1970, ApJ, 162, 405
Drury, L. O'C. 1983, Rep. Prog. Phys., 46, 973
Drury, L., O'C., Markiewicz, W. J., & Volk, H. J. 1989, A&A, 225, 179
Duric, N. 1988, Space Sci. Rev., 48, 73
———. 1989, in IAU Symp. 140, Galactic and Extragalactic Magnetic Fields, ed. R. Beck, P. P. Kronberg, & R. Wielebinski (Dordrecht: Kluwer)
Duric, N., & Glenn, J. 1991, in Proc. 22th Int. Cosmic Ray Conf., 4, 165
Duric, N., Seaquist, E. R., Crane, P. C., & Davis, L. E. 1986, ApJ, 304, 82
Duric, N., Viallefond, F., Goss, W. M., & van der Hulst, J. M. 1993, A&AS, 99, 217
Freedman, W. L., Wilson, C. D., & Madore, B. F. 1991, ApJ, 372, 455
Gaisser, T. K. 1990, Cosmic Rays and Particle Physics (New York: Cambridge Univ. Press)
Ginzburg, V. L., Khazan, Ya. M., & Ptuskin, V. S. 1980, Ap&SS, 68, 295
Gordon, S. 1994, Ph.D. thesis, Univ. New Mexico
Green, D. A. 1991, PASP, 103, 201
Harwit, M., & Pacini, F. 1975, ApJ, 200, L127
Haslam, C. G. T., Kearsey, S., Osborne, J. L., Phillips, S., & Stoffel, H. 1981, Nature, 289, 470
Helou, G., & Bicay, M. D. 1993, ApJ, 415, 93
Jones, T. W., & Kang, H. 1993, ApJ, 402, 560
Kang, H., & Drury, L. O.'C. 1990, ApJ, 399, 182
Long, K. S., Blair, W. P., Kirshner, R. P., & Winkler, P. F. 1990, ApJS, 72, 61
Longair, M. 1986, High Energy Astrophysics (Cambridge: Cambridge Univ. Press)
Pacholczyk, A. G. 1970, Radio Astrophysics (San Francisco: Freeman)
Smith, R. C. 1991, Ph.D. thesis, Harvard Univ.
van der Laan, H. 1962, MNRAS, 124, 179
Völk, H. J. 1989, A&A, 218, 67
Woltjer, L. 1972, ARA&A, 10, 129
Wunderlich, E., Klein, U., & Wielebinski, R. 1987, A&AS, 69, 487
Xu, C., Lisenfeld, U., & Völk, H. J. 1994, A&A, in press